

Silica Geothermometry Applications in the Taiwan Orogenic Belt

Chia-Mei Liu¹, Sheng-Rong Song^{2,*}, and Ching-Huei Kuo¹

¹Department of Geology, Chinese Culture University, Taipei, Taiwan, R.O.C.

²Institute of Geosciences, National Taiwan University, Taipei, Taiwan, R.O.C.

Received 10 September 2014, revised 20 January 2015, accepted 9 February 2015

ABSTRACT

The silica concentrations from 130 hot spring measurements were calculated and used to indicate the heat flow distribution in the active Taiwan orogenic belt. The heat flow spatial distribution seems to be controlled by the Taiwan arc-continent collision zone tectonic development. Two abnormally high silica heat flow regions, 160 and 190 mW m⁻², are identified in northeastern and southeastern Taiwan, respectively. In northeastern Taiwan, the Chingshui area, the data suggests that the anomalous heat flow distribution may be controlled mainly by hot fluids and faults. The highest heat flow in southeastern Taiwan may be generated by heat advection caused by a rapidly uplifting hot crust with a decreasing mature arc-continent collision zone exhumation rate. In addition, we estimated the exhumation rate in different tectonic zones in Southern Taiwan by applying fission track ages and silica heat flow values. The exhumation rates are 1.33, 1.72 - 3.87, and 0.51 - 1.74 mm yr⁻¹ in the tectonic zones around Taiwan for advanced, initial arc-continent collision and accretionary wedge deformation, respectively.

Key words: Taiwan, Regional heat flow, Arc-continent collision, Silica geothermometry

Citation: Liu, C. M., S. R. Song, and C. H. Kuo, 2015: Silica geothermometry applications in the Taiwan orogenic belt. *Terr. Atmos. Ocean. Sci.*, 26, 387-396, doi: 10.3319/TAO.2015.02.09.01(TT)

1. INTRODUCTION

It is well-known that a surface heat flow map is a useful tool for constructing regionally thermal regimes and revealing lithosphere and tectonic evolution thermal structure, especially for an active collision orogen. In general, a conventional heat flow map is derived from measuring subsurface rock temperatures and thermal conductivity. This method is common, direct and precise. However, drilling is time consuming and extremely costly. Fortunately, the silica geothermometry provides an inexpensive and quick alternative in comparison. Even though it is not as precise as the former method, it could produce sufficient information for understanding regional surface heat flow. Several studies have successively applied this technique in the USA, Egypt, Mexico, Anatolia, Fujian, and Australia (Swanberg and Morgan 1980; Prol-Ledesma and Juarez 1986; Vugrinovich 1987; Wan et al. 1989; Ilkışık 1995; Pirló 2002).

The island of Taiwan is located within an actively complex arc-continent collision. The Philippine Sea plate has been moving toward the WNW at about 80 mm yr⁻¹ resulting

in an ongoing mountain-building process (Yu et al. 1997). Due to the oblique collision, Taiwan exhibits various uplift rates (Liu 1982; Lan et al. 1990; Lundberg and Dorsey 1990; Liu et al. 2001; Lee et al. 2006) in all geological physiographic provinces of Taiwan Island from the north to the south, which include (1) the Coastal Range, the northern extend of Luzon arcs, consisting of sedimentary and volcanic rocks; (2) the Longitudinal Valley, the plate boundary between the Eurasian and Philippine Sea Plates; (3) the eastern Central Range, a pre-Tertiary metamorphic complex rock, containing the Yuli belt and western Tailuko belt; (4) the western Central Range composed of argillite, including the Backbone Range and the Hsuehshan Range belts; (5) the Western Foothills, the fold-and-thrust belt, consisting of clastic Oligocene-Pleistocene sedimentary rocks, and; (6) the Coastal Plain containing younger sediment deposits (Fig. 1) (Ho 1988). This oblique collision contributes to several unique general distribution patterns such as the age and metamorphic grade of Taiwan, increasing from the west to the east across Taiwan Island (Chen and Wang 1995) and the aseismic zone in the Central Range of Taiwan, which demonstrate the arc-continent collision zone complexity of Taiwan Island (Lin 2000). Several papers have been published that

* Corresponding author
E-mail: srsong@ntu.edu.tw

model the Taiwan arc-continent collision thermal structure and mountain-building mechanism (Barr and Dahlen 1989; Hwang and Wang 1993; Lin 2000; Song and Ma 2002; Zhou et al. 2003; Chi and Reed 2008), based on the conventional borehole measurements (Fig. 1a) (Lee and Cheng 1986). However, the sample distribution from previous studies is either restricted to certain areas or inadequately represented the area, especially for the Central Range of Taiwan.

The silica geothermometry (Swanberg and Morgan 1980), using hydro-geochemical data to estimate regional surface heat flow, is well suited to Taiwan due to its abundance of hot springs (Fig. 1b), which are distributed widely and easy to access for sampling purposes. In order to improve our understanding of the Taiwan mountain-building process in terms of thermal evolution, this study makes the first attempt at using the silica regional heat flow data to construct the possible thermal structures and controlling components in Taiwan.

2. MATERIAL AND METHOD

Enormous contributions have been made in silica temperature development which is based on the quartz solubility in water (Kennedy 1950; Bödvarsson 1960; Morey et al. 1962; Fournier and Rowe 1966; Mahon 1966). This geothermometer methodology has been proven the best method to calculate the subsurface temperature. There are four assumptions utilized in applying the silica geothermometer. They are (1) the equilibrium between water and rock is valid, (2) no other water body enters as water ascends to the surface,

(3) no precipitation occurs as the water reaches the surface, and (4) there is an unlimited supply for silicon dioxide. All collected samples were filtered through 0.22- μm cellulose filters in the field and stored in high-density polyethylene (HDPE). The silica concentration of these springs was measured using ICP-AES (Type Jobin-Yvon ULTIMA2).

One hundred and thirty spring samples were collected from all over Taiwan, as shown in Fig. 1b. All samples were analyzed to construct a regional silica heat flow map involving the three necessary processes. The silica concentration of these springs was measured using ICP-AES (Type Jobin-Yvon ULTIMA2). The silica concentrations were greater than 6 ppm (Fig. 2) indicating that quartz reached equilibrium with spring water (Morey et al. 1962). The silica temperature of these springs was then estimated using silica geothermometry (Fournier and Rowe 1966). To obtain regional representatives of the silica temperatures in this study, we set up the following criteria. If springs were located within the intersected region of two spring circles within 10 km radius (Fig. 3a), these springs were noted as one group (Fig. 3b). On the contrary, if the springs belonged to different physiographic provinces, they would not be averaged or grouped into separated blocks. Last, heat flow data were calculated using a linear equation, $T_{\text{SiO}_2} = mq + T_0$, where T_{SiO_2} is the silica geothermometry ($^{\circ}\text{C}$), q is heat flow (mW m^{-2}), T_0 is the long-term mean annual surface temperature, and m is the slope and designated as 0.68 (Swanberg and Morgan 1980). The slope m is a constant and corresponds to the minimum mean groundwater circulation depth at about 1.4 ± 0.5 km. Although these values are not fully confirmed, they are not

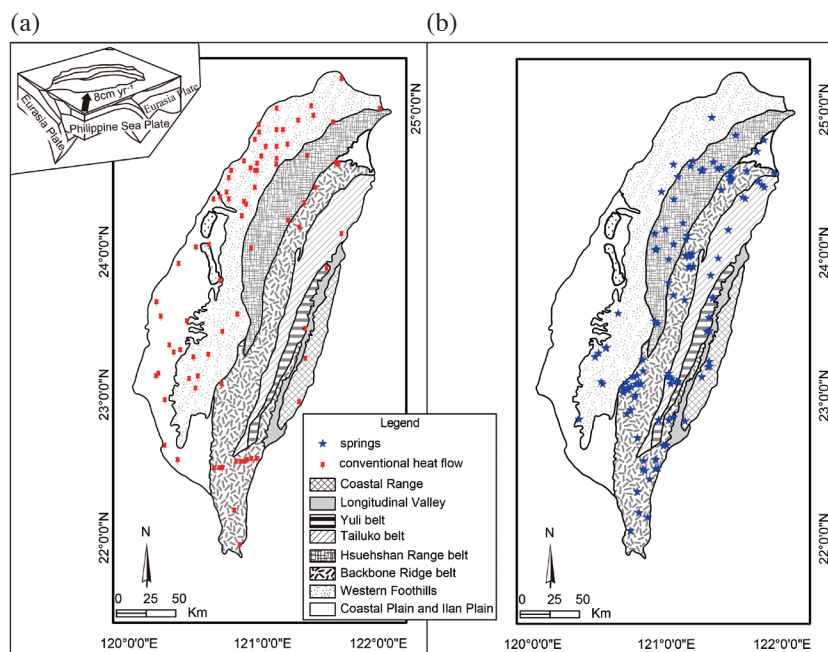


Fig. 1. (a) Most of the drill wells are located in the Western Foothills. (b) The spring area distribution is nearly all located in the Central Mountain Range. The left corner is the Philippine Sea plate moving towards the WNW at about 80 mm yr⁻¹.

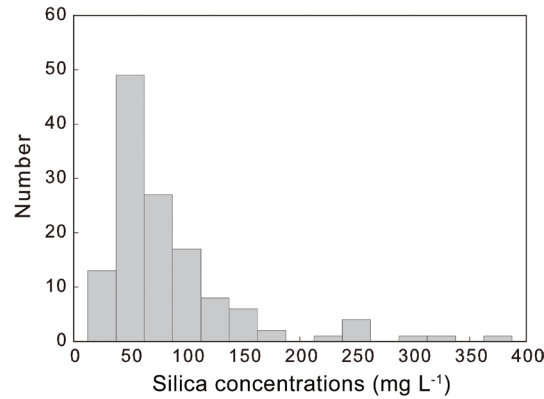


Fig. 2. All of the spring concentrations are higher than 6 ppm in Taiwan.

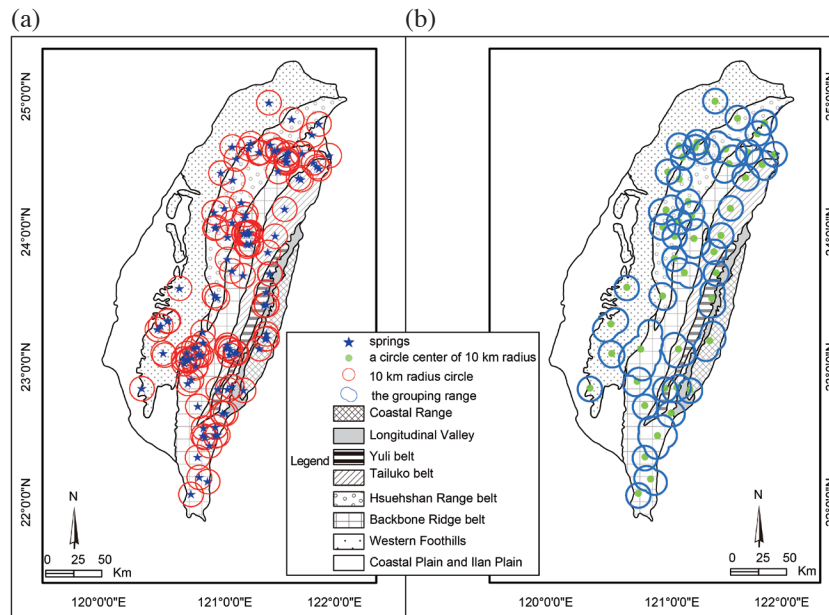


Fig. 3. (a) The red circles mean that the springs present a 10 km radius buffer. (b) The green point shows that the grouping and the blue range are the grouping results.

unrealistic (Swanberg and Morgan 1980). The long-term mean annual surface temperature (T_0) is 23.6°C in Taiwan based on Central Weather Bureau records from 1980 - 2008.

As was mentioned above, this study followed the silica geothermometry method steps to calculate the silica heat flow value of Taiwan. The silica heat flow map produced in this study was made using the Kriging method.

3. RESULTS

The estimated silica heat flow values for different physiographic provinces are 78 ± 23 mW m⁻² in Western Foothills; 117 ± 39 mW m⁻² in west Central Range, 126 ± 49 mW m⁻² in east Central Range; and 104 ± 13 mW m⁻² in Coastal Range (Table 1). The new Taiwan surface heat flow map is shown in

Fig. 4a and an AA' profile was made to exhibit the variations in North-South silica heat flow distribution. Two prominent peaks appear in the Chingshui area with value of 160 mW m⁻² and in the Chihpen area with the value of 190 mW m⁻², respectively (Fig. 4b). An interesting distribution pattern in northeastern-southwestern profile of Taiwan as the silica heat flow distribution increases from the Ilan Plain (100 mW m⁻²) to the Chingshui areas (160 mW m⁻²), then decreases to the Lushan area (100 mW m⁻²). As the profile turns to the south-eastern-northwestern direction the silica heat flow increases from the Lushan area (100 mW m⁻²) to the Chihpen area and reaches the peak (190 mW m⁻²). However, a lower silica heat flow area, about 80 mW m⁻² was found in Eastern Taiwan around the Haulien area, which is the location of a bended subducted slab of the Philippine Sea Plate (Lee et al. 2008).

Table 1. Springs of Taiwan and silica heat flow data.

Easting	Northing	Geological terrain	T (SiO₂)	σ	N	q
121.35915	24.99163	Hsuehshan Range belt	83.7	26.5	2	86.3
121.54144	24.86565	Backbone Ridge belt	123	-	1	145
121.76118	24.83065	Backbone Ridge belt	74.5	7.4	2	72.8
121.70379	24.75030	Western Foothills	60.2	-	1	51.7
121.84012	24.59909	Hsuehshan Range belt	101	-	1	112
121.73778	24.52437	Hsuehshan Range belt	95.2	-	1	103
121.62659	24.61447	Backbone Ridge belt	118	25.9	10	137
121.44244	24.64021	Hsuehshan Range belt	116	7.7	2	134
121.46948	24.53082	Hsuehshan Range belt	111	-	1	126
121.60413	24.42642	Backbone Ridge belt	98.5	25.6	15	108
121.28556	24.62088	Western Foothills	90.3	-	1	96.0
121.21119	24.69088	Western Foothills	84.3	-	1	87.2
121.06408	24.66414	Hsuehshan Range belt	90.4	9.1	4	96.2
121.09343	24.57811	Backbone Ridge belt	98.4	7.7	7	108
121.19544	24.65148	Hsuehshan Range belt	75.2	26.6	3	73.8
120.97392	24.47242	Backbone Ridge belt	128	41.6	2	152
121.06787	24.41865	Tailuko belt	130	34.3	6	154
121.47999	24.20287	Backbone Ridge belt	162	19.4	4	201
121.13814	24.25374	Backbone Ridge belt	148	29.1	8	182
120.96030	24.19108	Coastal Range	102	-	1	113
121.16733	24.14977	Backbone Ridge belt	132	16.6	5	157
121.06380	24.10505	Coastal Range	89.4	9.8	5	94.8
120.93302	24.06563	Yuli belt	136	13.1	3	164
121.02864	23.99754	Backbone Ridge belt	82.2	-	1	84.2
121.18466	23.98131	Backbone Ridge belt	159	22.1	2	196
121.40317	24.00239	Hsuehshan Range belt	109	7.6	2	124
121.34628	23.88246	Tailuko belt	114	13.0	3	131
121.02665	23.83447	Tailuko belt	85.4	-	1	88.8
121.10644	23.72870	Hsuehshan Range belt	113	-	1	130
121.36338	23.72652	Hsuehshan Range belt	115	5.2	2	133
121.32788	23.54022	Backbone Ridge belt	87.7	-	1	92.2
120.93134	23.55668	Hsuehshan Range belt	101	-	1	111
120.64344	23.62080	Hsuehshan Range belt	71.5	-	1	68.4
120.51413	23.34984	Backbone Ridge belt	56.2	-	1	45.9
120.52266	23.13301	Western Foothills	99.7	1.2	2	110
120.75515	23.16401	Hsuehshan Range belt	80.8	-	1	82.0
120.34949	22.87611	Western Foothills	64.2	-	1	57.7
121.05947	23.16419	Western Foothills	86.9	20.9	4	91.1
121.30966	23.22662	Backbone Ridge belt	140	45.1	8	163
120.72655	22.92739	Western Foothills	91.7	-	1	98.1
121.04581	22.88281	Hsuehshan Range belt	72.9	-	1	70.5
120.95103	22.87564	Western Foothills	54.5	-	1	43.3
121.15024	22.86661	Yuli belt	116	28.8	2	133
120.78875	22.74825	Tailuko belt	155	-	1	191

Note: N = number of observations; T = silica temperature in °C; σ is standard deviation; q = silica heat flow in mW m⁻².

Table 1. (Continued)

Easting	Northing	Geological terrain	T (SiO ₂)	σ	N	q
121.00131	22.69462	Tailuko belt	86.3	-	1	90.2
120.89134	22.52610	Tailuko belt	130	17.8	2	154
120.79125	22.37007	Western Foothills	72.6	-	1	70.0
120.83577	22.20701	Hsuehshan Range belt	84.7	-	1	87.8
121.40317	24.00239	Tailuko belt	45.5	-	1	30.1

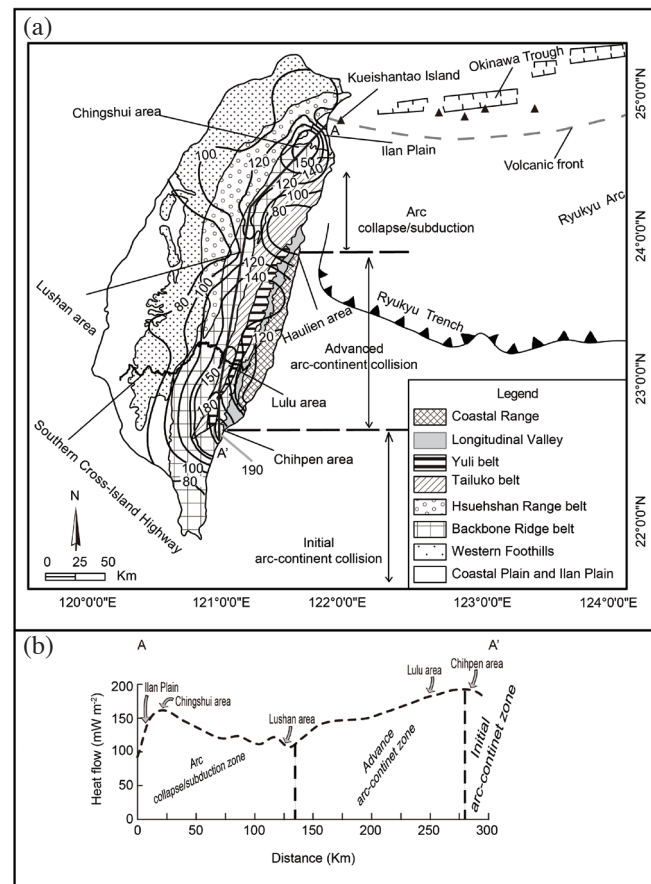


Fig. 4. (a) The silica heat flow contour map (this map does not include the Tatun Volcano Group) in three tectonic zones of Taiwan. Based on the geologic and geophysical characteristics, Taiwan can be divided into three tectonic zones including the arc collapse subduction, the advanced and the arc collapse collision zones (Huang et al. 2000). Triangles denote submarine volcanoes. (b) The regional silica heat flow distribution AA' profile is across Taiwan Island from north to south. In the arc collapse/subduction zone, the peak value is located at the Chingshui area and decreases northeastwardly to the Ilan Plain and southwestwardly to the Lushan area. In the arc-continent collision zone the highest value is located at the Chihpen area and declines to the north.

4. DISCUSSION

4.1 Comparison Conventional and Silica Heat Flow

Previous studies have shown some unjustified high heat flow values, greater than 300 mW m⁻² distributed in Taiwan (Fig. 5), particularly, in the Central Mountain Range (Lee and Cheng 1986). The heat flow spatial distribution in this study was significantly better than those found for the Western Foothills and Coastal Plain (Fig. 1). The average

silica and conventional heat flow values are 110 ± 41 and 125 ± 105 mW m⁻², respectively (Figs. 6a and b). Some conventional data were too high, more than 300 mW m⁻², to be reasonable in the Central Mountain Range. Similar results were found for silica with reasonable conventional heat flow in different physiographic provinces, as shown in Fig. 6.

According to the silica geothermometry method, the standard silica geo-temperature deviation value is usually less than 25°C to represent more accuracy and reliable silica

heat flow value in one block (Swanberg and Morgan 1980). In this study, most standard deviation values for silica geotemperature were less than 25°C (Table 1). In addition, the silica results and most quality conventional heat flow values were comparable. For example, the silica and conventional heat flow values were 91 and 100 mW m^{-2} (Huang 1990), in the Kuantzuling area of the Western Foothills, respectively. The Jinlun area in the Central Mountain Range presented silica and conventional heat flow values of 170 and 140 mW m^{-2} (Gou 2008), respectively. The silica heat flow values are 160 mW m^{-2} and the conventional values are from $164 - 192 \text{ mW m}^{-2}$ in the Chingshui area of the Central Mountain Range (Huang et al. 1986). As a result this silica geothermometry method is adequate for revealing regional heat flow distributions.

4.2 The Silica Heat Flow Map Variation and its Interpretation

Two anomalies with higher silica heat flow are located at the Chingshui and Chihpen areas and can be identified in Fig. 4b. Their values are 1.5 - 2 times higher than the average continental heat flows in the rest of the world. In general, the surface heat flows are contributed by basement, radiogenic elements, exhumation, burial, fault/fluid, magma, and tectonic components (Blackwell 1978; Bodell and Chapman 1982; Lachenbruch et al. 1985; Armstrong

and Chapman 1998). Understanding these components provides information for the regionally thermal regimes needed that reveal the thermal structure. This study discusses what

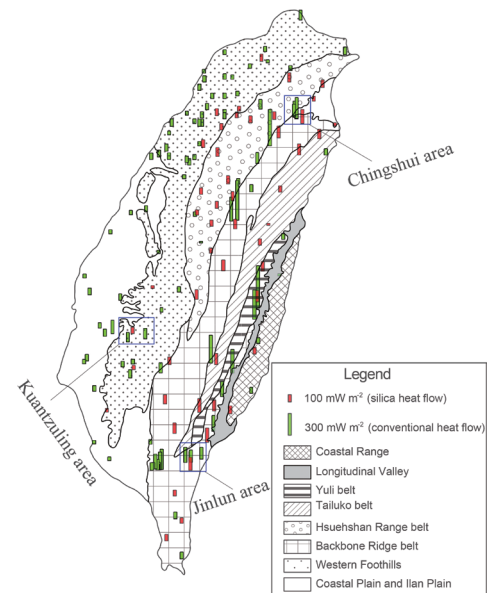


Fig. 5. This shows that both heat flow values are consistent in the Kuantzuling area, the sedimentary terrain of the Western Foothills and the Jinlun and Chingshui areas, the metamorphic terrain of the Central Mountain Range.

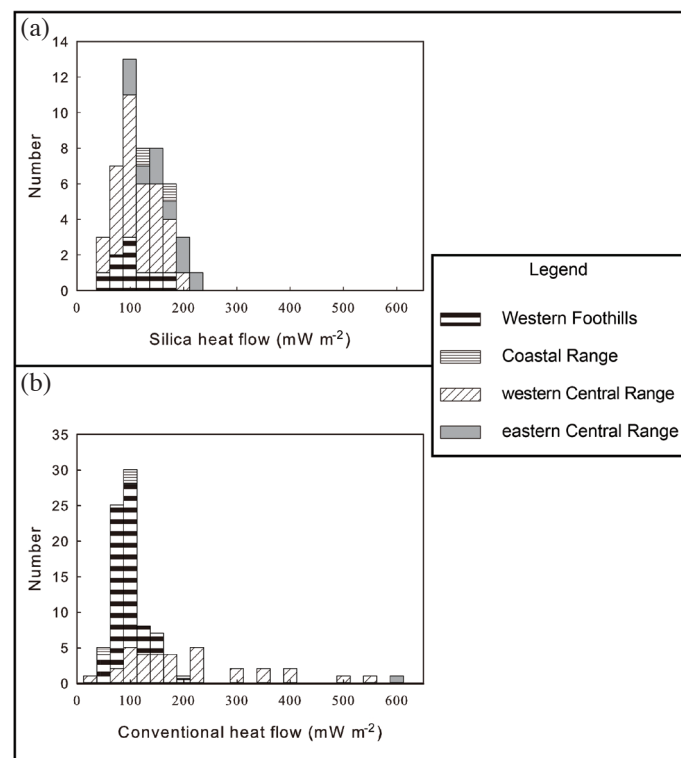


Fig. 6. (a) This histogram presents that the silica heat flow values and their numbers in different geological terrain. (b) Showing the conventional heat flow data-set. Some heat flow values are higher than 300 mW m^{-2} in the Central Range.

unique components control the anomalously high heat flow in the Taiwan orogen.

In northeastern Taiwan our results show that a heat source exists beneath the Chingshui area of the Ilan Plain (Fig. 7a). This existing heat source is supported by other methods and results, the helium isotopic ratio of soil gases, seismic data, geomagnetic and magneto telluric data and borehole information (Yu and Tsai 1979; Yang et al. 2005; Lan et al. 2006; Tong et al. 2008).

Few researches have investigated the mechanism that generates this heat anomaly. In fact the Philippine Sea Plate subducts northward under the Eurasian Plate, producing the Ryukyu Trench-Okinawa Trough system. The Okinawa Trough is generally recognized as a back-arc basin in an arc-continent collision system. However, it is not just a simple back-arc basin but rather an embryonic rift zone based on major and trace elements from volcanic rocks in the Southernmost Part of the Okinawa Trough (SPOT), (Chung et al. 2000). It has been shown to extend southwestward from the Okinawa Trough into the Ilan Plain using geodetic monitoring and micro-earthquake results (Liu 1995; Lai et al. 2009). The SPOT extension has been shown to cause the normal faults and magmatic intrusion in the arc collapse/subduction region (Chiang 1976). Thus, the origin of abnormally high silica heat flow in the Chingshui area likely results from the southwestward propagation of hot fluids from the Okinawa Trough into the Ilan Plain (Fig. 7a).

The silica heat flow spatial distribution shows a decreasing distribution from the Chingshui to the Lushan areas southwestwardly and the Ilan Plain northeastwardly (Fig. 6b). Chang (1989) showed a similar radiogenic spatial distribution for the Hsuehshan Range and the Backbone Ridge belts suggesting that both of them should produce the same heat generation near the surface. The decreasing silica heat flow pattern is likely caused by a heat transfer from below. A boundary fault, the Lishan fault, and many subsidiary faults between the Backbone Ridge and the Hsuehshan Range belts have been recognized in this region (Fig. 7a) (Chiang 1976; Lee et al. 1997). A fault can act as a channel that assists heat/fluid transfer. As a result, the Lishan and other faults in the Ilan Plain likely function as conduits that transfer heat and fluid southwestward and northeastward from Chingshui to the Lushan areas and the Ilan Plain (Fig. 7a).

An aseismic zone was recognized by Lin (2000) based on the seismicity distribution of the Central Mountain Range. With conventional heat flow data numerical modeling, this aseismic zone was attributed to a faster exhumation rate along the Southern Cross-Island Highway (Lin 2000). In southeastern Taiwan a different mechanism, exhumation, was proposed as the major contributor to anomalous surface heat flow. In addition, the upward extrusion of the Central Mountain Range has been proposed as the exhumation process explaining fanning structures with inverted metamorphism (Yui and Chu 2000). Our results showed that the ex-

humation is most likely located at the Chihpen area, 55 km south of the Southern Cross-Island Highway. GPS analysis showed strong dilatation within the Chihpen area (Hsu et al. 2009) and the zircon fission track displays the fastest exhumation rate since 0.4 Ma in the same area. These data indicate that buoyant hot materials are exhuming upward beneath the Chihpen area now (Fig. 7b).

The oblique arc-continent collision in Taiwan propagates southwardly, generating different exhumation rates in various tectonic zones. The exhumation rates for Taiwan were calculated using the fission track data under the constant geothermal gradient values ($30^{\circ}\text{C km}^{-1}$) (Lee et al. 2006). The gradient temperature seems underestimated for a reasonable exhumation rate calculation in Southern Taiwan, leading to exhumation rate miscalculation. It seems logical to have more reliable geothermal gradients for estimating the exhumation rate in Southern Taiwan. We, therefore, combined the silica heat flow and fission track dating to estimate the thermal

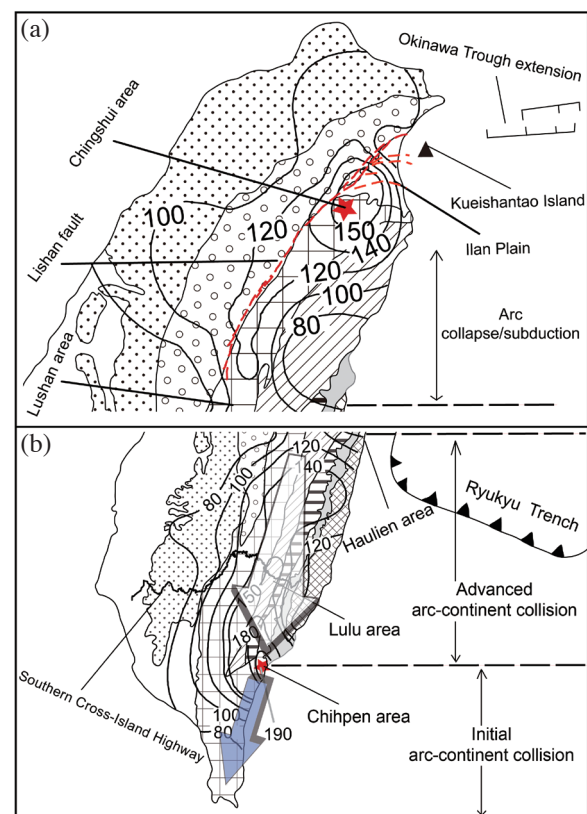


Fig. 7. The schematic map illustrates the abnormal silica heat flow distribution. (a) In the arc collapse/subduction of northern Taiwan, the heat source is beneath the Chingshui area, and the heat transmits to the Lushan area along the Lishan fault. The solid star indicates the hot fluids/heat source beneath the Chingshui area, and the dashed line shows the fault traces. (b) The silica heat flow distribution is consistent with the Southern Taiwan tectonic zones that indicate propagation toward southernmost Taiwan. The solid star shows that the fastest exhumation rate is located in the Chihpen area. The gray arrow is the propagation direction of the increasing silica heat flow and the blue arrow is the propagation direction of the decreasing silica heat flow.

evolution of Southern Taiwan. This is because the heat decays with time and higher heat flow exists in active tectonic zones than in stable areas according to the Fourier's law of heat flow (Carslaw and Jaeger 1986). The silica heat flows are estimated between 120 - 190 mW m⁻² and increase from the advanced to initial arc-continent collision zones. In addition, the zircon and apatite fission track dating display partial annealing and total reset zones in Southern Taiwan (Fuller et al. 2006). According to the fission track partial and total reset zones, cooling (the tectonic zones of advance and initial arc-continent collision) and accretionary ages (accretionary wedge deformation zone) (Huang et al. 2000; Fuller et al. 2006) can be distinguished. The estimated geothermal gradient values are about 55, 71, and 39°C km⁻¹ in the advanced, initial arc-continent collision, and accretionary wedge deformation tectonic zones using the silica heat flow, respectively. Furthermore, the fission track ages of apatite are 1.5, 0.4 - 0.9, and 1.6 - 5.5 Ma, and the corresponding silica geotemperature values are about 130, 160, and 100°C at depths of 1.9 km in the advanced, initial arc-continent collision and accretionary wedge deformation tectonic zones, respectively. We combined the geothermal gradient values and apatite fission track ages to estimate the exhumation rate of Southern Taiwan (Tsao 1996). We estimated the exhumation rate in different tectonic zones at about 1.33 mm yr⁻¹ in the advanced arc-continent collision zone, 1.72 - 3.87 mm yr⁻¹ in the initial arc-continent collision zone and 0.51 - 1.74 mm yr⁻¹ in the accretionary wedge deformation zone, respectively (Fig. 8). These values are much lower than the previously published exhumation rates (Lee et al. 2006). In light of the discrepancy between this study and others, further discussion on the exhumation rate of Taiwan is needed.

5. CONCLUSIONS

This paper constructed a heat flow map of Taiwan and

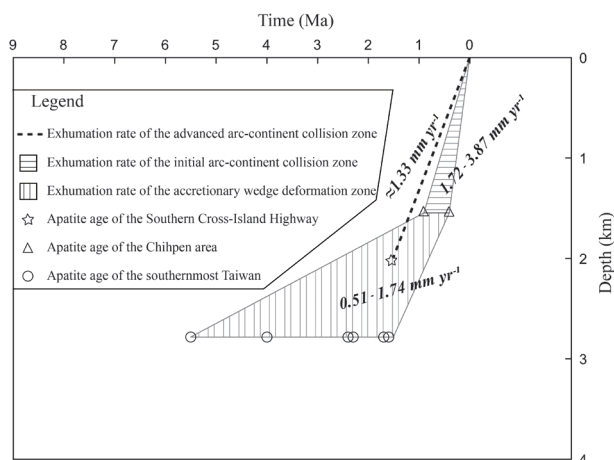


Fig. 8. The exhumation rate in different tectonic zone of the Southern Taiwan.

examined three major controlling factors (1) hot fluids, (2) faults, and (3) exhumation which dominate the surface heat flow in Taiwan. The Okinawa Trough opening produces a heat fluid source beneath the Chingshui area with this heat transferring into the Lushan area and the Ilan Plain along the Lishan and other faults. The thermal anomaly around the Chihpen area, however, results from rapid exhumation in the initial arc-continent collision zone.

Acknowledgements We thank Wei Lo and Yi-Gui Lin for their help with collecting samples for this work. We are grateful to En-Chao Yeh and the Editors for their constructive comments and help in improving this manuscript. This research is indebted to the National Science Council of Taiwan under grants NSC 96-2627-M-002-011, NSC 98-2627-M-002-002, and NSC 102-2116-M-034-002.

REFERENCES

- Armstrong, P. A. and D. S. Chapman, 1998: Beyond surface heat flow: An example from a tectonically active sedimentary basin. *Geology*, **26**, 183-186, doi: 10.1130/0091-7613(1998)026<0183:BSHFAE>2.3.CO;2. [Link]
- Barr, T. D. and F. A. Dahlen, 1989: Brittle frictional mountain building: 2. Thermal structure and heat budget. *J. Geophys. Res.*, **94**, 3923-3947, doi: 10.1029/JB094iB04p03923. [Link]
- Blackwell, D. D., 1978: Heat flow and energy loss in the Western United States. In: Smith, R. B. and G. P. Eaton (Eds.), *Cenozoic Tectonics and Regional Geophysics of the Western Cordillera*, Geological Society of America Memoir, Vol. 152, Geological Society of America, Boulder, 175-208, doi: 10.1130/MEM152-p175. [Link]
- Bodell, J. M. and D. S. Chapman, 1982: Heat flow in the north-central Colorado Plateau. *J. Geophys. Res.*, **87**, 2869-2884, doi: 10.1029/JB087iB04p02869. [Link]
- Bödvarsson, G., 1960: Exploration and exploitation of natural heat in Iceland. *Bull. Volcanol.*, **23**, 241-250, doi: 10.1007/BF02596651. [Link]
- Carslaw, H. S. and J. C. Jaeger, 1986: *Conduction of Heat in Solids*, 2nd edition, Oxford Science Publications, 520 pp.
- Chang, H. C., 1989: Radioactivity and heat generation of rocks in the Taiwan region. Ph.D. Thesis, National Central University, Taoyuan, Taiwan, 159 pp. (in Chinese)
- Chen, C. H. and C. H. Wang, 1995: Explanatory notes for the metamorphic facies map of Taiwan. Special Publication of the Central Geological Survey, Vol. 2, Central Geological Survey, MOEA, New Taipei, Taiwan, 32 pp. (in Chinese)
- Chi, W. C. and D. L. Reed, 2008: Evolution of shallow, crustal thermal structure from subduction to collision: An example from Taiwan. *Geol. Soc. Am. Bull.*, **120**, 679-690, doi: 10.1130/B26210.1. [Link]

- Chiang, S. C., 1976: Seismic study in the Ilan Plain. *Min. Tech.*, **14**, 215-221. (in Chinese)
- Chung, S. L., S. L. Wang, R. Shinjo, C. S. Lee, and C. H. Chen, 2000: Initiation of arc magmatism in an embryonic continental rifting zone of the southernmost part of Okinawa Trough. *Terr. Nova*, **12**, 225-230, doi: 10.1046/j.1365-3121.2000.00298.x. [[Link](#)]
- Fournier, R. O. and J. J. Rowe, 1966: Estimation of underground temperatures from the silica content of water from hot springs and wet-steam wells. *Am. J. Sci.*, **264**, 685-697, doi: 10.2475/ajs.264.9.685. [[Link](#)]
- Fuller, C. W., S. D. Willett, D. Fisher, and C. Y. Lu, 2006: A thermomechanical wedge model of Taiwan constrained by fission-track thermochronometry. *Tectonophysics*, **425**, 1-24, doi: 10.1016/j.tecto.2006.05.018. [[Link](#)]
- Gou, T. R., 2008: Metamorphic type geothermal characteristics study by using integrated geophysical methods—Example from Jinlun geothermal. Ph.D. Thesis, National Central University, Taoyuan, Taiwan, 130 pp. (in Chinese)
- Ho, C. S., 1988: An Introduction to the Geology of Taiwan: Explanatory Text of the Geologic Map of Taiwan, 2nd edition, Central Geological Survey, MOEA, New Taipei City, Taiwan, 192 pp.
- Hsu, Y. J., S. B. Yu, M. Simons, L. C. Kuo, and H. Y. Chen, 2009: Interseismic crustal deformation in the Taiwan plate boundary zone revealed by GPS observations, seismicity, and earthquake focal mechanisms. *Tectonophysics*, **479**, 4-18, doi: 10.1016/j.tecto.2008.11.016. [[Link](#)]
- Huang, C. Y., P. B. Yuan, C. W. Lin, T. K. Wang, and C. P. Chang, 2000: Geodynamic processes of Taiwan arc-continent collision and comparison with analogs in Timor, Papua New Guinea, Urals and Corsica. *Tectonophysics*, **325**, 1-21, doi: 10.1016/S0040-1951(00)00128-1. [[Link](#)]
- Huang, L. S., 1990: Preliminary study on the subsurface temperature and geothermal gradients of the late Cenozoic basin in Western Taiwan. *Bull. Cent. Geol. Surv.*, **6**, 117-144. (in Chinese)
- Huang, S. T., K. C. Chuang, and J. W. Yuan, 1986: Mineralogy of hydrothermal alteration and heat flow system in the Chingshui geothermal field, I-Lan. *Pet. Eng.*, **9**, 80-81. (in Chinese)
- Hwang, W. T. and C. Wang, 1993: Sequential thrusting model for mountain building: Constraints from geology and heat flow of Taiwan. *J. Geophys. Res.*, **98**, 9963-9973, doi: 10.1029/92JB02861. [[Link](#)]
- Ilkışık, O. M., 1995: Regional heat flow in western Anatolia using silica temperature estimates from thermal springs. *Tectonophysics*, **244**, 175-184, doi: 10.1016/0040-1951(94)00226-Y. [[Link](#)]
- Kennedy, G. C., 1950: A portion of the system silica-water. *Econ. Geol.*, **45**, 629-653, doi: 10.2113/gsecon-geo.45.7.629. [[Link](#)]
- Lachenbruch, A. H., J. H. Sass, and S. P. Galanis Jr., 1985: Heat flow in southernmost California and the origin of the Salton Trough. *J. Geophys. Res.*, **90**, 6709-6736, doi: 10.1029/JB090iB08p06709. [[Link](#)]
- Lai, K. Y., Y. G. Chen, Y. M. Wu, J. P. Avouac, Y. T. Kuo, Y. Wang, C. H. Chang, and K. C. Lin, 2009: The 2005 Ilan earthquake doublet and seismic crisis in north-eastern Taiwan: Evidence for dyke intrusion associated with on-land propagation of the Okinawa Trough. *Geophys. J. Int.*, **179**, 678-686, doi: 10.1111/j.1365-246X.2009.04307.x. [[Link](#)]
- Lan, C. Y., T. Lee, and C. W. Lee, 1990: The Rb-Sr isotopic record in Taiwan gneisses and its tectonic implication. *Tectonophysics*, **183**, 129-143, doi: 10.1016/0040-1951(90)90412-2. [[Link](#)]
- Lan, T. F., T. F. Yang, Y. Sano, H. F. Lee, and C. C. Fu, 2006: Invasion of mantle-derived fluids into I-Lan plain, NE Taiwan from southwest part of the Okinawa Trough: Evidence of Helium isotopes in soil gases. American Geophysical Union, Fall Meeting 2006, abstract #V23C-0647, San Francisco, American.
- Lee, C. R. and W. T. Cheng, 1986: Preliminary heat flow measurements in Taiwan. Fourth Circum-Pacific Energy and Mineral Resources Conference, Singapore.
- Lee, J. C., J. Angelier, and H. T. Chu, 1997: Polyphase history and kinematics of a complex major fault zone in the northern Taiwan mountain belt: The Lishan Fault. *Tectonophysics*, **274**, 97-115, doi: 10.1016/S0040-1951(96)00300-9. [[Link](#)]
- Lee, Y. H., C. C. Chen, T. K. Liu, H. C. Ho, H. Y. Lu, and W. Lo, 2006: Mountain building mechanisms in the Southern Central Range of the Taiwan Orogenic Belt - From accretionary wedge deformation to arc-continental collision. *Earth Planet. Sci. Lett.*, **252**, 413-422, doi: 10.1016/j.epsl.2006.09.047. [[Link](#)]
- Lee, Y. H., G. T. Chen, R. J. Rau, and K. E. Ching, 2008: Coseismic displacement and tectonic implication of 1951 Longitudinal Valley earthquake sequence, eastern Taiwan. *J. Geophys. Res.*, **113**, B04305, doi: 10.1029/2007JB005180. [[Link](#)]
- Lin, C. H., 2000: Thermal modeling of continental subduction and exhumation constrained by heat flow and seismicity in Taiwan. *Tectonophysics*, **324**, 189-201, doi: 10.1016/S0040-1951(00)00117-7. [[Link](#)]
- Liu, C. C., 1995: The Ilan plain and the southwestward extending Okinawa Trough. *J. Geol. Soc. China*, **38**, 229-242.
- Liu, T. K., 1982: Tectonic implication of fission-track ages from the Central Range, Taiwan. *Proc. Geol. Soc. China*, **25**, 22-37.
- Liu, T. K., S. Hsieh, Y. G. Chen, and W. S. Chen, 2001: Thermo-kinematic evolution of the Taiwan oblique-collision mountain belt as revealed by zircon fission

- track dating. *Earth Planet. Sci. Lett.*, **186**, 45-56, doi: 10.1016/S0012-821X(01)00232-1. [[Link](#)]
- Lundberg, N. and R. J. Dorsey, 1990: Rapid Quaternary emergence, uplift, and denudation of the Coastal Range, eastern Taiwan. *Geology*, **18**, 638-641, doi: 10.1130/0091-7613(1990)018<0638:RQEUAD>2.3.CO;2. [[Link](#)]
- Mahon, W. A. J., 1966: Silica in hot water discharged from drillholes at Wairakei, New Zealand. *New Zealand J. Sci.*, **9**, 135-144.
- Morey, G. W., R. O. Fournier, and J. J. Rowe, 1962: The solubility of quartz in water in the temperature interval from 25° to 300°C. *Geochim. Cosmochim. Acta*, **26**, 1029-1043, doi: 10.1016/0016-7037(62)90027-3. [[Link](#)]
- Pirlo, M. C., 2002: The silica heat flow interpretation technique: Application to continental Australia. *J. Volcanol. Geotherm. Res.*, **115**, 19-31, doi: 10.1016/S0377-0273(01)00306-7. [[Link](#)]
- Prol-Ledesma, R. M. and M. G. Juarez, 1986: Geothermal map of Mexico. *J. Volcanol. Geotherm. Res.*, **28**, 351-362, doi: 10.1016/0377-0273(86)90030-2. [[Link](#)]
- Song, T. R. A. and K. F. Ma, 2002: Estimation of the thermal structure of a young orogenic belt according to a model of whole-crust thickening. *GSA Spec. Pap.*, **358**, 121-136, doi: 10.1130/0-8137-2358-2.121. [[Link](#)]
- Swanberg, C. A. and P. Morgan, 1980: The silica heat flow interpretation technique: Assumptions and applications. *J. Geophys. Res.*, **85**, 7206-7214, doi: 10.1029/JB085iB12p07206. [[Link](#)]
- Tong, L. T., S. Ouyang, T. R. Guo, C. R. Lee, K. H. Hu, C. L. Lee, and C. J. Wang, 2008: Insight into the geothermal structure in Chingshui, Ilan, Taiwan. *Terr. Atmos. Ocean. Sci.*, **19**, 413-424, doi: 10.3319/TAO.2008.19.4.413(T). [[Link](#)]
- Tsao, S., 1996: The geological significances of illite crystallinity, zircon fission-track ages, and K-Ar ages of metasedimentary rocks. Ph.D. Thesis, National Taiwan University, Taipei, Taiwan, 272 pp. (in Chinese)
- Vugrinovich, R., 1987: Regional heat flow variations in the northern Michigan and Lake Superior region determined using the silica heat flow estimator. *J. Volcanol. Geotherm. Res.*, **34**, 15-24, doi: 10.1016/0377-0273(87)90089-8. [[Link](#)]
- Wan, T., Y. Tong, and W. Zheng, 1989: Thermal Structure of the Lithosphere in Fujian, China. *J. Geophys. Res.*, **94**, 1888-1894, doi: 10.1029/JB094iB02p01888. [[Link](#)]
- Yang, T. F., T. F. Lan, H. F. Lee, C. C. Fu, P. C. Chuang, C. H. Lo, C. H. Chen, C. T. A. Chen, and C. S. Lee, 2005: Gas compositions and helium isotopic ratios of fluid samples around Kuishantao, NE offshore Taiwan and its tectonic implications. *Geochem. J.*, **39**, 469-480.
- Yu, S. B. and Y. B. Tsai, 1979: Geomagnetic anomalies of the Ilan Plain, Taiwan. *Petrol. Geol. Taiwan*, **16**, 19-27.
- Yu, S. B., H. Y. Chen, and L. C. Kuo, 1997: Velocity field of GPS stations in the Taiwan area. *Tectonophysics*, **274**, 41-59, doi: 10.1016/S0040-1951(96)00297-1. [[Link](#)]
- Yui, T. F. and H. T. Chu, 2000: 'Overtuned' marble layers: Evidence for upward extrusion of the Backbone Range of Taiwan. *Earth Planet. Sci. Lett.*, **179**, 351-361, doi: 10.1016/S0012-821X(00)00119-9. [[Link](#)]
- Zhou, D., H. S. Yu, H. H. Xu, X. B. Shi, and Y. W. Chou, 2003: Modeling of thermo-rheological structure of lithosphere under the foreland basin and mountain belt of Taiwan. *Tectonophysics*, **374**, 115-134, doi: 10.1016/S0040-1951(03)00236-1. [[Link](#)]